Available online at www.sciencedirect.com

SciVerse ScienceDirect

Ceramics International 39 (2013) 2147–2152

CERAMICS INTERNATIONAL

www.elsevier.com/locate/ceramint

Short communication

Fabrication and properties analysis of C_f–CNT/SiC composite

Zhihui Hu[a,b], Shaoming Dong[a,*], Jianbao Hu[a,b], Bo Lu[a,b]

[a]*State Key Laboratory of High Performance Ceramics and Superfine Microstructure, Shanghai Institute of Ceramics, Chinese Academy of Sciences, Shanghai 200050, China*

[b]*Institute of Graduate, Chinese Academy of Sciences, Beijing 100039, China*

Received 15 April 2012; received in revised form 23 July 2012; accepted 23 July 2012
Available online 29 August 2012

Abstract

2D C_f–CNT/SiC composite was fabricated by the hand-lay-up-molding–PIP method, with carbon fiber coated with carbon nanotubes (CNTs) as reinforcement. Chemical vapor deposition (CVD) was conducted to obtain a homogeneous dispersion of CNTs on carbon fiber with Al_2O_3 as a catalyst promoter, which adhered to the carbon fiber together with a catalyst precursor impregnated in $Fe(NO_3)_3 \cdot 9H_2O$ and $Al(NO_3)_3 \cdot 6H_2O$ solutions. The results showed that the interlaminar shear strength (ILSS) of C_f–CNT/SiC composite increased by 100.9% and the thermal conductivity in the orientation perpendicular and parallel to the carbon fiber direction increased by 24.3% and 78% respectively compared to the C_f/SiC composite.

Keywords: Carbon fiber; Carbon nanotube; Silicon carbide matrix composite

1. Introduction

Carbon nanotubes (CNTs) have attracted much attention as potential reinforcements for composites due to their excellent mechanical, electrical, and thermal properties [1–6]. However, the natural tendency of CNTs is to exist as agglomerates for their strong surface forces [7–9], which limits their application as uniformly dispersed reinforcements. Recently, researchers have attempted molecular level mixing [10], sol–gel process [11,12], heterocoagulation [13,14], spray drying [15,16] and chemical vapor deposition (CVD) [7,17] to effectively disperse the CNTs in the ceramic matrix. All of these CNTs dispersion techniques have evinced varying degrees of success with some limitations.

This study suggested that the growth of CNTs on carbon fiber (C_f) by CVD provided an excellent alternative, not only to "disperse" CNTs in the composite but also obtain a "dense" coating. Hence, the objective of the present study is to synthesize C_f–CNT／SiC composite with high density CNT dispersion and excellent interlaminar shear strength (ILSS) and thermal conductivity.

2. Material and methods

Hybrid reinforcement of carbon fiber grafted with CNTs (C_f–CNTs) was synthesized by CVD with Al_2O_3 as the catalyst promoter. Carbon fibers T300 were made to undertake nitride acid treatment, and were then impregnated in $Fe(NO_3)_3 \cdot 9\ H_2O$ and $Al(NO_3)_3 \cdot 6\ H_2O$ solutions. The CNTs were grafted on the carbon fibers as described by Fan Z et al. [18].

The obtained C_f–CNTs hybrid reinforcement was infiltrated with phenolic resin. Then the reinforcement was pressed, which was then infiltrated with xylene and polycarbonsilane (PCS) slurry several times to fabricate the C_f–CNT/SiC composites after pyrolysis and solidification.

The ILSS test was conducted on an INSTRON 5566 (Instron Corp., Canton, MA) universal testing machine using double-notched shear specimens (DNS) [19] as shown in Fig. 1. The microstructure of the fracture surfaces was characterized by a JEOL JEM-6700 Hitachi

*Corresponding author. Tel.: +86 21 52415207; fax: +86 21 52413903.
E-mail address: smdong@mail.sic.ac.cn (S. Dong).

0272-8842/$ - see front matter © 2012 Elsevier Ltd and Techna Group S.r.l. All rights reserved.
http://dx.doi.org/10.1016/j.ceramint.2012.07.077

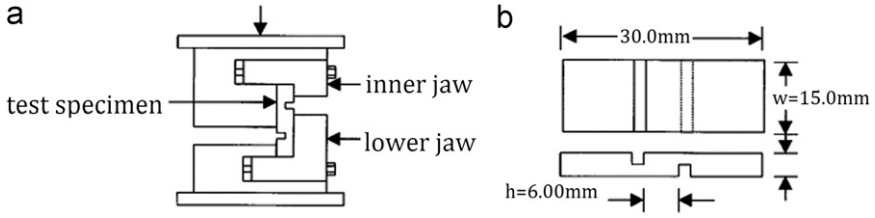

Fig. 1. (a) Schematic illustration of an ILSS test fixture and (b) Test specimen geometry.

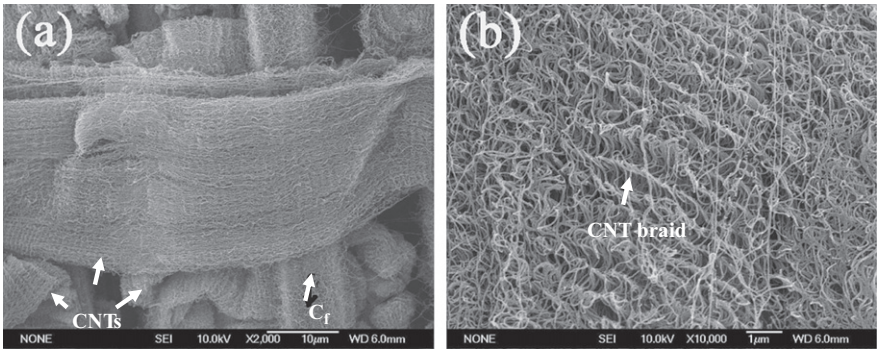

Fig. 2. SEM image of CNTs on carbon fiber with the Al_2O_3 as the catalyst promoter.

scanning electron microscope (SEM) with a field-emission gun operated at 10 kV.

Thermal conductivity was measured by a laser flash technique with a laser conductometer (Shanghai Institute of Ceramics, Chinese Academy of Sciences, Shanghai, China). The thermal diffusivity measurement of C_f–CNT/SiC composites was done with the orientation perpendicular or parallel to the carbon fiber direction.

3. Results and discussion

3.1. Growth of braid CNT on carbon fiber and mechanism

Fig. 2 reveals the SEM image of CNTs on carbon fibers with Al_2O_3 as the catalyst promoter. As is shown in Fig. 2a, carbon fiber, which is marked with an arrow, is surrounded by a lot of CNTs. Besides, the length of CNTs shown in Fig. 2a can reach 1 μm. Fig. 2b is the high resolution SEM image of Fig. 2a, and it is obviously demonstrated that CNT braid can be obtained with Al_2O_3 as the catalyst promoter. Therefore, it is hopeful to enhance the composite interfacial bond strength to fabricate C_f–CNT/SiC composite with excellent ILSS and thermal conductivity.

Fig. 3 shows the XRD patterns of carbon fibers after different CVD processes. Fig. 3I displays the XRD pattern of carbon fibers after different CVD processes with no catalyst promoter. Fig. 3Ia shows the XRD pattern of carbon fiber without any treatment; Fig. 3Ib shows the XRD pattern of the carbon fiber that has adsorbed the catalyst precursor; Fig. 3Ic shows the XRD pattern of the carbon fiber that has been impregnated with the catalyst precursor solution and has undertaken thermal treatment at 750 °C under Ar gas atmosphere for 30 min; Fig. 3Id shows the XRD pattern of the carbon fiber that has been impregnated with the catalyst precursor solution and has undertaken thermal treatment at 750 °C under H_2 gas atmosphere for 30 min; Fig. 3Ie shows the XRD pattern of the carbon fiber grafted with carbon nanotubes; Fig. 3II shows the XRD patterns of carbon fibers after different CVD processes, and Al_2O_3 was used as the catalyst promoter; Fig. 3IIa shows the XRD pattern of the carbon fiber that has adsorbed the catalyst and the catalyst promoter precursor; Fig. 3IIb shows the XRD pattern of the carbon fiber that has been impregnated with the catalyst and catalyst promoter precursor solution and has undertaken thermal treatment at 750 °C under Ar gas atmosphere for 30 min; Fig. 3IIc shows the XRD pattern of the carbon fiber that has been impregnated with the catalyst and catalyst promoter precursor solution and has undertaken thermal treatment at 750 °C under H_2 gas atmosphere for 30 min; and Fig. 3IId shows the XRD pattern of the carbon fiber grafted with carbon nanotubes.

It is indicated in Fig. 3I that the main components of carbon fiber which has been impregnated with $Fe(NO_3)_3 \cdot 9H_2O$ solution are C and α-Fe_2O_3; some Fe_3O_4 appears in the carbon fibers after 30 min heat treatment at 750 °C; then Fe_2C came up after catalyst reduction in hydrogen ambience at 750 °C for 30 min. Finally, all oxides of iron were substituted by Fe_2C and Fe_3C after the growth of CNTs on carbon fibers. Besides, it is revealed in Fig. 3Ia and b that the diffraction peak of (100) of crystal surface of graphite structure became weaker as the CVD process went on, while the diffraction peak of (400) of crystal surface of graphite structure nearly disappears. As a result, it is evident that the graphite

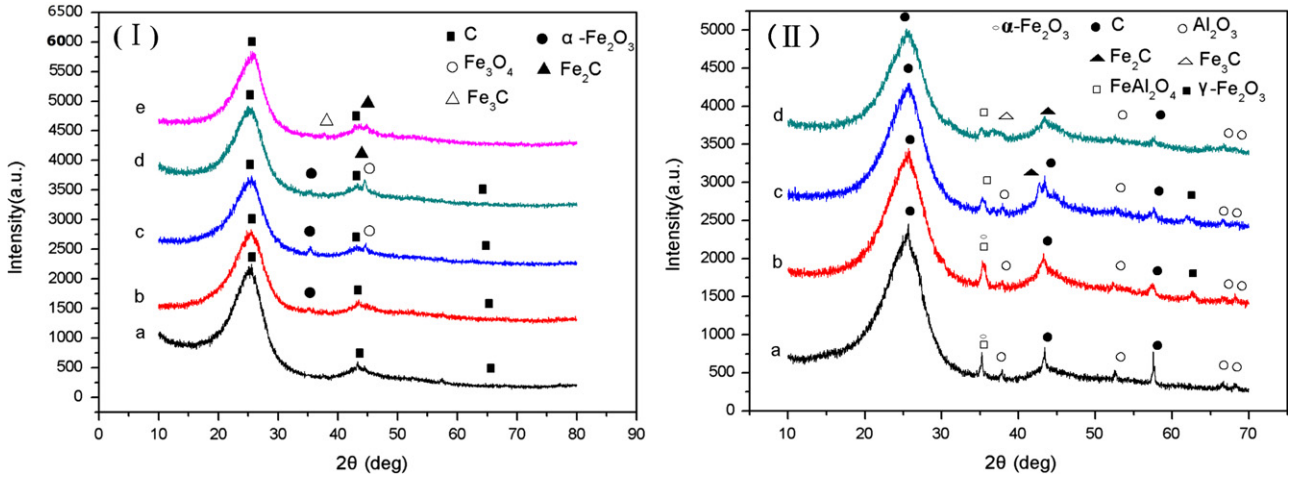

Fig. 3. XRD images of carbon fiber after different CVD processes: (I) Without any the catalyst promoter; (II) Using Al_2O_3 as the catalyst promoter.

Table 1
ILSS and thermal conductivity of 2D C_f/CNTs–SiC composite and 2D C_f–SiC composite.

	Fiber content (%)	Density (g/cm^3)	Open porosity (%)	ILSS (Mpa)	Thernal conductivity λ (W/(m K))	
					$\lambda_\perp$	$\lambda_\parallel$
C_f–SiC composite	54	1.62	7.19	21.4	4.47	7.3
C_f/CNT–SiC composite	54	1.66	6.6	43	3.07	13

structure of carbon fiber was gradually destructed as the CVD process went on.

As is shown in Fig. 3II, the main components of carbon fiber which have been impregnated with $Fe(NO_3)_3 \cdot 9H_2O$ and $Al(NO_3)_2 \cdot 6H_2O$ solutions are C, Al_2O_3, $FeAl_2O_4$ and α-Fe_2O_3. There is no Fe_3O_4 but γ-Fe_2O_3 is present in the carbon fibers after 30 min heat treatment at 750 °C, then Fe_2C came up after catalyst reduction in hydrogen ambience at 750 °C for 30 min. Finally, all oxides of iron were substituted by Fe_2C and Fe_3C after the growth of CNTs on carbon fibers. Besides, it is revealed in Fig. 3IIa–d that the diffraction peak of the compound of $FeAl_2O_4$ became weaker as the CVD process went on.

Therefore, the following conclusions as follows can be obtained by comparing Fig. 3I and II: (1) the graphite structure of carbon fiber can be protected from destruction with Al_2O_3 as the catalyst promoter; (2) when there was no catalyst promoter, α-Fe_2O_3 was first reduced to Fe_3O_4, and it was then reduced to Fe [12]. However, α-Fe_2O_3 can be directly reduced to Fe when using Al_2O_3 as the catalyst promoter; (3) with the help of Al_2O_3, the paramagnetic α-Fe_2O_3 can turn into ferromagnetic γ-Fe_2O_3, which has higher activity than α-Fe_2O_3 for the growth of CNTs on the carbon fiber [13]; (4) when Al_2O_3 was used as the catalyst promoter Al^{3+} subsitituted the Fe^{3+} of Fe_2O_3 and formed $FeAl_2O_4$, which becomes a solid solution together with Fe_2O_3. And the solid solution can inhibit the growth of crystal. The formation of $FeAl_2O_4$ is useful for the reconstruction of α-Fe, which makes the crystal faces of (100), (111), and (110) have the same activity. The $FeAl_2O_4$ can also be a barrier for the interdiffusion between carbon fibers and catalyst [14–16]. Therefore, when using Al_2O_3 as the catalyst promoter, braids of CNTs can be obtained with the graphite structure of carbon fiber to be protected from destruction.

3.2. ILSS and thermal conductivity of C_f–CNTs/SiC composite

The density, open porosity, ILSS, and thermal conductivity of 2D C_f/SiC composite and 2D C_f–CNT/SiC composite are listed in Table 1. Compared to C_f/SiC composite, the density of C_f–CNT/SiC composite was increased by 3.7%, open porosity decreased by 7.0%, ILSS increased by 100.9%, and thermal conductivity in the orientation perpendicular and parallel to the carbon fiber direction increased by 24.3% and 78% respectively. Therefore, the addition of CNTs on one hand improved the ILSS of SiC matrix composite efficiently, and on the other hand, it brought more marked improvement of thermal conductivity parallel to the carbon fiber direction than perpendicular to the carbon fiber direction as the CNT braid was grown in the orientation parallel to the carbon fiber direction as shown in Fig. 2a.

3.3. Discussion of mechanism

The fracture section of the 2D C_f–CNT/SiC composite and 2D C_f/SiC composite after double-notch shear (DNS) was tested to explain the improvement of ILSS and

thermal conductivity of the 2D C_f–CNT/SiC composite. And what's more, a detailed study of the surface morphologies and composition of carbon fibers in different CVD stages was made in the research.

Figs. 4 and 5 show the fracture surface morphologies of 2D C_f/SiC and 2D C_f–CNT/SiC composite samples in DNS test, respectively. As is shown in Fig. 4a, the carbon fibers were easily fractured under external force, which suggests that carbon fibers have been damaged when the composite was fabricated. Additionally, a smooth fracture section can be found in Fig. 4b, which reveals that the bonding strength of carbon fiber to the ceramic matrix was poor. Some pores can be found in Fig. 4c, which resulted in the poor bonding strength of carbon fiber to the ceramic matrix while the thermal conductivity of composites decreased. In contrast, it is more difficult for the carbon fibers using the C_f–CNTs as reinforcement to fracture as shown in Fig. 5a than it is for those shown in Fig. 4a. The fracture section in Fig. 5b and c is rougher than that in Fig. 4, which suggests that a strong interface bonding exists between the carbon fiber and ceramic matrix, and it is attributed to the addition of CNTs, which can be proved by Fig. 5d. Therefore, the increase in of ILSS of 2D C_f–CNT/SiC composite by 100.9% than that of 2D C_f/SiC should be attributed to the strong interface bonding between the carbon fiber and ceramic matrix.

The morphologies of carbon fiber surface with different processes are demonstrated in Fig. 6. Fig. 6a shows the SEM image of the carbon fiber that has adsorbed the catalyst and catalyst promoter precursor; Fig. 6b reveals the SEM image of the carbon fiber that has been impregnated with the catalyst and catalyst promoter precursor solution and has undertaken thermal treatment at 750 °C under Ar gas atmosphere for 30 min; Fig. 6c demonstrates the SEM image of the carbon fiber that has been impregnated with the catalyst and catalyst promoter precursor solution and has undertaken thermal treatment at 750 °C under H_2 gas atmosphere for 30 min; and Fig. 6d displays the SEM image of the carbon fiber grafted with carbon nanotubes. From Fig. 6a–d, conclusions can be made as follows: (1) a thick layer of catalyst and catalyst promoter, which may have a low thermal conductivity according to the XRD results as

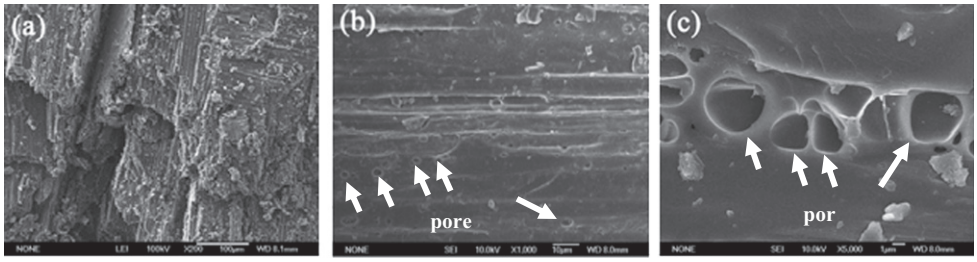

Fig. 4. Fracture surface morphologies of 2D C_f–SiC composite samples after shear test.

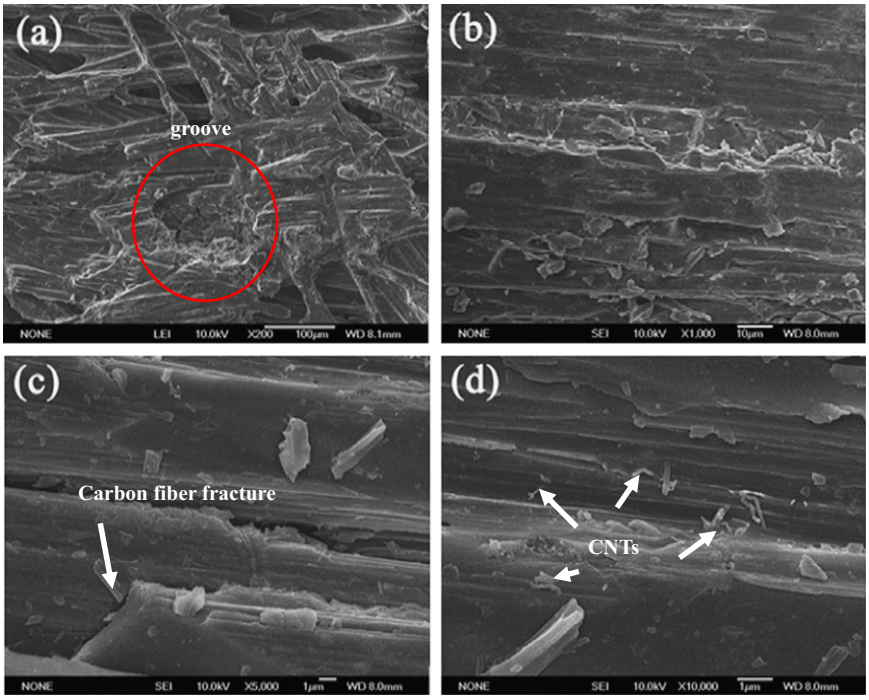

Fig. 5. Fracture surface morphologies of 2D C_f/CNT–SiC composite samples after shear test.

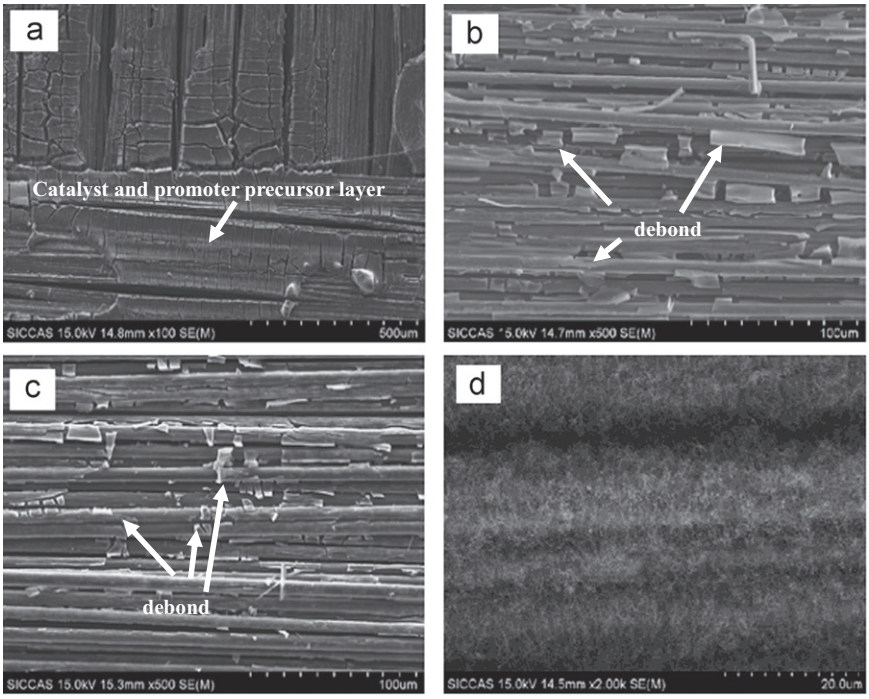

Fig. 6. Morphologies of carbon fibers after different CVD processes: (a) the SEM image of the carbon fiber that has adsorbed the catalyst precursor; (b) the SEM image of the carbon fiber that has been impregnated with the catalyst precursor solution and has undertaken thermal treatment at 750 °C under Ar gas atmosphere for 30 min; (c) the SEM image of the carbon fiber that has been impregnated with the catalyst precursor solution and has undertaken thermal treatment at 750 °C under H_2 gas atmosphere for 30 min; and (d) the SEM image of the carbon fiber grafted with carbon nanotubes.

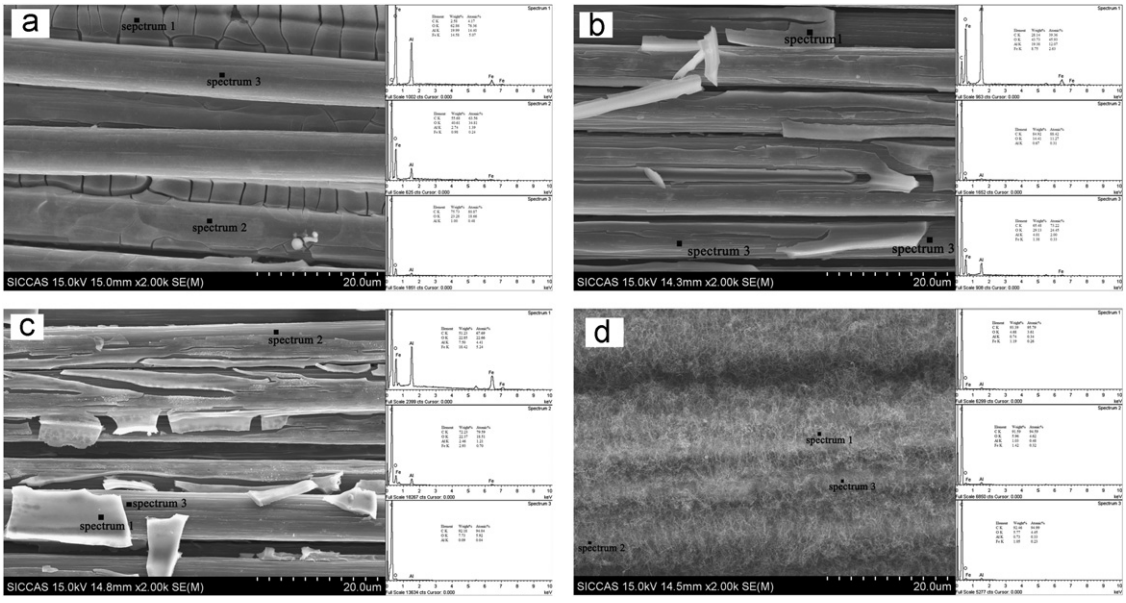

Fig. 7. Phase analysis of the surface of carbon fibers after different CVD processes: (a) the carbon fiber that has adsorbed the catalyst precursor; (b) the carbon fiber that has been impregnated with the catalyst precursor solution and has undertaken thermal treatment at 750 °C under Ar gas atmosphere for 30 min; (c) the carbon fiber that has been impregnated with the catalyst precursor solution and has undertaken thermal treatment at 750 °C under H_2 gas atmosphere for 30 min; and (d) the carbon fiber grafted with carbon nanotubes.

mentioned above has adhered to the carbon fiber limiting the improvement of thermal conductivity of 2D C_f–CNT/SiC composite; (2) the bondings of carbon fibers, the layer of catalyst and catalyst promoter are weak as the layer is shed off gradually as the CVD process went on, which affected the ILSS of 2D C_f–CNT/SiC composite.

Fig. 7 shows the surface phase of carbon fibers after different CVD processes. Fig. 7a shows the SEM image of the carbon fiber that has adsorbed the catalyst and catalyst promoter precursor; Fig. 7b reveals the SEM image of the carbon fiber that has been impregnated with the catalyst and catalyst promoter precursor solution and has undertaken

thermal treatment at 750 °C under Ar gas atmosphere for 30 min; Fig. 7c demonstrates the SEM image of the carbon fiber that has been impregnated with the catalyst and catalyst promoter precursor solution and has undertaken thermal treatment at 750 °C under H_2 gas atmosphere for 30 min; and Fig. 7d displays the SEM image of the carbon fiber grafted with carbon nanotubes. It can be found in Fig. 7a–d that carbon fibers in each stage of CVD process have high oxygen concentration, such that the carbon fiber and CNTs may be easily damaged when the composite has been fabricated, and this resulted in the liability to damage of carbon fibers and CNTs. As a result, a thin layer of CNTs can be found on the fracture surface and the carbon fiber was easily fractured.

4. Conclusions

In order to obtain homogeneous dispersion of CNTs and enhance the interaction of carbon fiber/matrix at the interface, CNTs were grown on carbon fibers via the CVD technique with Al_2O_3 as the catalyst promoter. CNT braid has been grafted on carbon fibers to synthesize the C_f–CNT hybrid reinforcement, and the promoting mechanism has been discussed in detail . The 2D C_f–CNT/SiC and 2D C_f/SiC composites have also been fabricated by the hand-lay-up-molding–PIP method. Compared to that of the C_f/SiC composite, the ILSS of C_f–CNT/SiC composites increased by 100.9% and thermal conductivity in orientations perpendicular and parallel to the carbon fiber direction increased by 24.3% and 78% respectively. Finally, it is found that the improvement of ILSS and thermal conductivity is attributed to the uniform dispersion of CNTs and toughening mechanisms, such as CNT bridging, crack deflection and strong interaction between carbon fibers and silicon carbide matrix at interfaces.

Acknowledgments

This project was funded partly by the National Natural Science Foundation of China (Grant no. 51002170) and the Innovation Program of Shanghai Institute of Ceramics, Chinese Academy of Sciences (Grant no. Y12ZC6160G).

References

[1] J.N. Coleman, U. Khan, W.J. Blau, Y.K. Gun'ko, Small but strong: a review of the mechanical properties of carbon nanotube–polymer composites, Carbon 44 (2006) 1624–1652.
[2] J.P.S. Delmottea, A. Rubioc, Mechanical properties of carbon nanotubes: a fiber digest for beginners, Carbon 40 (2002) 1729–1734.
[3] P. Kim, L. Shi, A. Majumdar, P.L. McEuen, Thermal transport measurements of individual multiwalled nanotubes, Physical Review Letters 87 (2001) 215502–215514.
[4] J.P. Lu, Elastic properties of single and multilayered nanotubes, The Journal of Physics and Chemistry of Solids 58 (1997) 1649–1652.
[5] M.M.J. Treacy, T.W. Ebbesen, J.M. Gibson, Exceptionally high Young's modulus observed for individual carbon nanotubes, Nature 381 (1996) 678–680.
[6] M. Yu, O. Lourie, M.J. Dyer, K. Moloni, T.F. Kelly, R.S. Ruoff, Strength and breaking mechanism of multiwalled carbon nanotubes under tensile load, Science (New York, NY) 287 (2000) 637–640.
[7] K. Balani, T. Zhang, A. Karakoti, W.Z. Li, S. Seal, A. Agarwal, In situ carbon nanotube reinforcements in a plasma-sprayed aluminum oxide nanocomposite coating, Acta materialia 56 (2008) 571–579.
[8] R.B. Pipes, P. Hubert, J.P. Salvetat, L. Zalamea, Flexural deflection as a measure of van der Waals interaction forces in the CNT array, Composites Science and Technology 66 (2006) 1125–1131.
[9] Y.S. Song, J.R. Youn, Influence of dispersion states of carbon nanotubes on physical properties of epoxy nanocomposites, Carbon 43 (2005) 1378–1385.
[10] S.I. Cha, K.T. Kim, K.H. Lee, C.B. Mo, S.H. Hong, Strengthening and toughening of carbon nanotube reinforced alumina nanocomposite fabricated by molecular level mixing process, Scripta Materialia 53 (2005) 793–797.
[11] C.B. Mo, S.I. Cha, K.T. Kim, K.H. Lee, S.H. Hong, Fabrication of carbon nanotube reinforced alumina matrix nanocomposite by sol–gel process, Materials Science and Engineering A 395 (2005) 124–128.
[12] R. Poyato, A.L. Vasiliev, N.P. Padture, H. Tanaka, T. Nishimura, Aqueous colloidal processing of single-wall carbon nanotubes and their composites with ceramics, Nanotechnology 17 (2006) 1770–1777.
[13] S. Lei, Z.Y. Feng, Z. Chan, L. JI, Heterocoagulation system assisted adsorption of carbon nanotubes on alumina for toughening ceramics, Journal of Reinforced Plastics and Composites 27 (2008) 245–253.
[14] J. Sun, L. Gao, Development of a dispersion process for carbon nanotubes in ceramic matrix by heterocoagulation, Carbon 41 (2003) 1063–1068.
[15] K. Balani, A. Agarwal, Process map for plasma sprayed aluminum oxide–carbon nanotube nanocomposite coatings, Surface and Coatings Technology 202 (2008) 4270–4277.
[16] K. Balani, S.R. Bakshi, Y. Chen, T. Laha, A. Agarwal, Role of powder treatment and carbon nanotube dispersion in the fracture toughening of plasma-sprayed aluminum oxide–carbon nanotube nanocomposite, Journal of Nanoscience and Nanotechnology 7 (2007) 1–10.
[17] E. Flahaut, A. Peigney, C. Laurent, C. Marlie, F. Chastel, A. Rousset, Carbon nanotube–metal oxide nanocomposites: microstructure, electrical conductivity and mechanical properties, Acta Materialia 48 (2000) 3803–3812.
[18] Z. Fan, C. Wu, J.H. Chen, Growth of carbon nanotubes on the surface of carbon fibers, Carbon 46 (2008) 380–383.
[19] J.J. Fang, T.W. Chou, Characterization of interlaminar shear strength of ceramic matrix composites, Journal of the American Ceramic Society 76 (1993) 2539–2548.